

# Heat Flow Analysis and Stress Analysis of Laser-Welded Lap Joints under the Same Fatigue Loading Using the Finite Element Method

Ankush Tiwari<sup>1</sup>, Sharad Kumar Chandrakar<sup>2</sup>, Ashish Pradhan<sup>3</sup>, Abhishek Kumar<sup>4</sup>

<sup>1,2,3,4</sup>SSGI Bhilai

---

**Abstract:** Laser welding technology is used widely in many industrial welds such as spaceflight, aviation and automobile production. The fatigue behavior of the laser-welded structures is complicated by many factors intrinsic to the nature of laser-welded joints. In this study two types of specimens were employed for the welding and the fatigue tests using finite element analysis. The first is the transverse directional laser-welded specimen, which is perpendicular to fatigue load, using 1 mm thick SPCC sheets. The second is the longitudinal directional laser-welded specimen, which is parallel to fatigue load. For these two types of specimens, a tensile shear fatigue test was performed and result found that the fatigue strength of the transverse lap laser-welded joint is higher than that of the longitudinal lap laser-welded joint.

## 1. INTRODUCTION

Laser welding technology is used widely in many industrial welds such as spaceflight, aviation and automobile production [1]. Because of its low heat input, high welding speed, high penetration, easy automation and high accuracy. One of the great advantages of laser welding is that it produces keyhole type welding. The high penetration and narrow heat-affected zone of laser welding results from this keyhole type welding because of the high power density. However, even with all the potential advantages of laser welding, there is still hesitancy in using this technology in the primary structural components.

Laser-welded structures are often subjected to dynamic service loads ranging from the cyclic fluctuations to the completely random loads. The laser-welded lap joints suffer from defects resulting in the notch effect and surface cracks, residual stress, etc. The fatigue strength of the laser-welded lap joints is reduced significantly because of these defects. Therefore, the strength of laser welded structures can be defined in terms of the fatigue strength of the joints. The fatigue behavior of the laser-welded structures is complicated by many factors intrinsic to the nature of laser-welded joints.

Many researchers have conducted studies to estimate fatigue strength in welds. They considered the geometrical stress

concentration effects [2], the metallurgy change [3], the size and location of the welding discontinuities [4]. Recently, studies on fatigue behavior considering the residual stress in the resistance spot welding was performed by Yang et al. [5].

Normally, residual stresses introduced in laser-welded lap joints are a consequence of compatible thermal strains caused by heating and cooling cycles during the welding process. These affect the fatigue behavior of the laser-welded structures. Especially, tensile residual stress of the order of yield strength may exist in as-welded structures along weld bead. And this may cause a detrimental effect on the fatigue behavior of the welded structures [6]. The distribution of residual stress in and surrounding a laser-welded joint is complex and depends on a number of factors, including material composition, thickness, applied restraint, and welding direction [7]. When fatigue load is applied to a laser-welded joint that contains residual stress, the applied and residual stresses will combine. Especially, in the laser-welded joint, which has welding direction parallel or perpendicular to fatigue load, the fatigue behavior of the laser-welded joint considering residual stresses will be different.

In the manufacturing technology sphere, this study aims to use finite element analysis to predict the fatigue life of laser-welded joints subjected to the interaction effects of welding direction and residual stress. Residual stress welds in weldments were calculated using thermo-elastic-plastic finite element analysis and the equivalent fatigue stress, taking into account the residual stress effect is obtained. Fatigue life, which is affected by the residual stress field, is then determined. The finite element program ABAQUS [8], along with a few user subroutines, is employed for the analysis; comparison of the calculated results with experimental data shows the accuracy and validity of the proposed method.

## 2. LASER WELDING OF LAP JOINT

The material being examined is SPCC steel sheet, which is similar to cold-rolled steel plates (A366 in ASTM norm). The

thickness of steel sheet used for the laser-welded lap joint is 1.0 mm. The chemical composition in weight percentage and the mechanical properties of the testing specimen are shown in Table 1. SPCC steel sheet is generally used for fabricating vehicle bodies, oil fan and electrical appliances. Lap joints are mainly used in sheet fabrication and in consumer goods such as cars, washing machines, etc. Recent trends toward economically fabricating vehicle structures have led to the implementation of laser-welded lap joint instead of resistance spot welding. The laser welding used in this study is performed using a continuous CO<sub>2</sub> laser beam with a maximum power of 4 kW. The fixed-part/mobile welding head assembly is equipped with an accurate positioning and clamping device, under CNC (computer numerical control) control. Argon gas of flow rate 30 L/min is provided for the shielding of the lap joint. Fig. 1 shows the schematic diagram of a laser-welded specimen. The specimen size is 180 x 140 x 1 mm<sup>3</sup> and the size of lap joint is 320 x 40 x 1 mm<sup>3</sup> in the transverse direction welding and 260 x 40 x 1 mm<sup>3</sup> in the longitudinal direction welding as shown in Fig. 1.

**Table 1: Chemical composition and mechanical properties of SPCC steel sheet**

Chemical composition (wt %)					Mechanical properties		
C	Si	Mn	P	S	Yield strength (M Pa)	Tensile strength (M Pa)	Elongation (%)
0.02	0.01	0.16	0.013	0.007	210	320	40

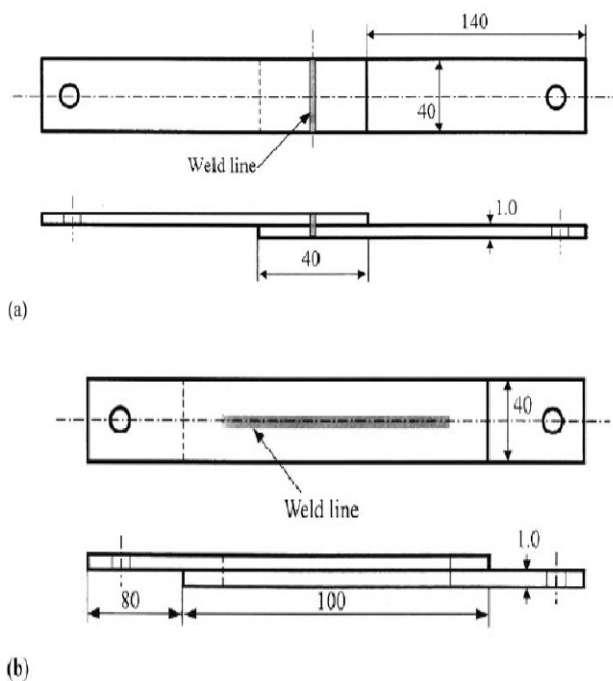


**Fig 1. Schematic diagrams of specimens: (a) transverse direction welding, (b) longitudinal direction welding.**

**Table 2 Laser welding condition for specimen type**

Specimen type	Welding speed (m/min)	Laser power (kW)	Focus position
Transverse direction welding	2	2	Surface (0 mm)
Longitudinal direction welding	2	2	Surface (0 mm)

To avoid the notch at the edge of specimen, the samples are prepared using the standard procedure including cutting and milling. Before laser welding, the surface of the SPCC steel sheet is cleaned with acetone solution in order to remove dirt and oil. Laser welding is performed using the welding condition given in Table 2. After the layered SPCC steel sheets are clamped by the jig, these are welded simultaneously so as to obtain equal weld quality for the transverse and longitudinal directions.

### 3. FINITE ELEMENT ANALYSIS

The laser welding process is characterized by the highly collimated and concentrated beam energy. This process makes it difficult to provide an accurate measurement of temperature and strain near the fusion zone, so that finite element analysis seems to be more comprehensive. The finite element method is used to determine equivalent fatigue stress in the laser-welded lap joint under fatigue load. Using the data of temperature distribution of the heat flow analysis the thermo-elastic-plastic stress analysis is performed during complete cooling to the ambient temperature. Then in order to calculate equivalent fatigue stress the elastic-plastic stress analysis with the residual stress effect is carried out.

The finite element program ABAQUS [8], along with a few user subroutines, is employed in order to obtain numerical results of thermal history and residual stress field. The three-dimensional finite element modeling is used in the analysis of both the heat flow and stress in the lap joint. The finite element mesh for the lap joint is shown in Fig. 2. Each model is meshed with eight-node quadrilateral elements. Fusion zone and HAZ exhibit severe stress and temperature gradient. Therefore, fine mesh is used within and around the fusion zone and the HAZ and the outer mesh is coarse. When the direction of laser welding is longitudinal, half of the full region in the lap joint is modeled because longitudinal laser welding is symmetric to x-axis. In the case of transverse laser welding, full region of lap joint is modeled.

#### Heat flow analysis

To determine the residual stresses of the laser weldment, the thermal history in the laser-welded lap joint is calculated using transient heat flow analysis. Compared to arc welding process, the laser welding process is normally performed in a keyhole mode with very high-power density beams and high velocity, which leads to the formation of a vapor capillary through the

material. The energy transfer from the laser beam to the work piece is simulated by the heat flux in order to exhibit the keyhole effect in the fusion zone. There are two typical heat flux distributions; the Gaussian profile and the line-like source (line source). The geometric features of the Gaussian distribution are expressed by the following equation:

$$q(r) = \frac{3Q}{\pi r^2} \exp \left\{ -3 \left( \frac{r}{\bar{r}} \right)^2 \right\},$$

where  $r$  is the radial distance from the laser beam center,  $S r$  is the characteristic radius (defined as the radius at which the intensity of the laser beam falls to 5% of the maximum intensity) and  $Q$  is the power transferred into the workpiece. In the case of the Gaussian profile, the heat flux on the top surface of the workpiece is distributed at the melting zone ( $y = 0$ ). The heat flux of the line source perpendicular to the plate plane at the melting zone ( $y = 0$ ) is employed as shown in Fig. 3. Two types of heat flux flow into a workpiece along the welding line. In this work, the material properties of the SPCC steel sheet that are required for the heat flow analysis are thermal conductivity, specific heat, density and latent heat. The material properties are considered to be dependent on temperature. To incorporate these material properties into the simulation, these are obtained from the literature [9]. The initial condition for the entire solution domain is room temperature. On surfaces, only natural convection is considered as a boundary condition.

Thermal stress and residual stress are calculated using the results of the thermal history obtained by heat flow analysis. Thermo-elastic-plastic finite element analysis is carried out. The material properties that are required for the thermal and residual stress analysis are elastic modulus, plastic modulus, yield strength and thermal expansion coefficient. These material properties are considered to be dependent on temperature [9]. The solution domain for stress analysis is the same as that for heat flow analysis shown in Fig. 3. The boundary condition of stress analysis is shown in Fig. 3. Displacements and rotations of the nodes are constrained as shown in Fig. 3. For longitudinal laser welding, since the symmetry condition around the  $x$ -direction is satisfied, the displacement of  $y$ -direction at  $x = 0$  is fixed and a half-model is adopted as the solution domain. When an external load is applied to the laser welding lap joint, the resultant multiaxial stress distribution, including residual stress effects, can be determined. After thermal and residual stress was conducted, the stress analysis is performed for the respective external fatigue loads in the same solution domain. The boundary condition is identical to the condition of a tensile-shear fatigue test.

### Fatigue strength

Generally, the relation between fatigue life of mild steel and ultimate tensile strength is as follows [10]:

$$S = 10^C N^b \quad \text{for} \quad 10^3 < N < 10^6,$$

Where  $S$  is alternating stress,  $N$  is the number of cycles to failure (lifetime), and the material constants  $C$  and  $b$  are determined as follows:

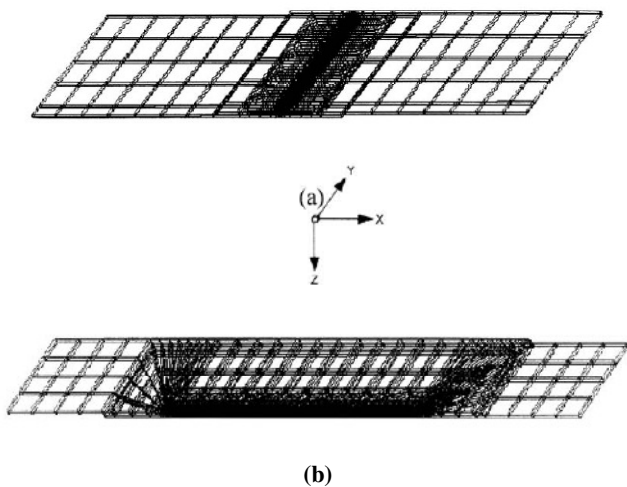


Fig. 2. Mesh generation for finite element analysis: (a) transverse direction welding, (b) longitudinal direction.

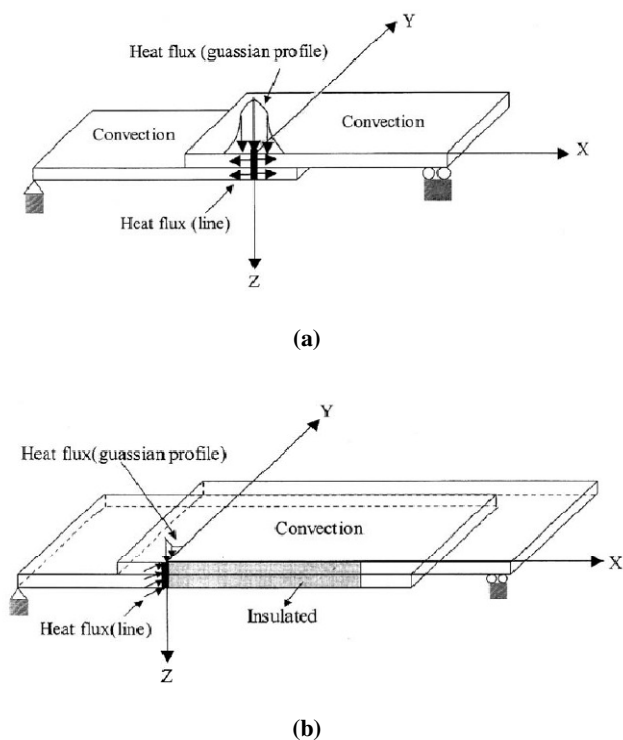


Fig. 3. Boundary condition of heat flow and stress analysis: (a) boundary condition of transverse direction welding, (b) boundary condition of longitudinal direction welding.

$$C = \log_{10} \frac{(S_{1000})^2}{S_e}, \quad b = -\frac{1}{3} \log_{10} \frac{S_{1000}}{S_e}$$

Here,  $S_{1000} = 0.9S_u$ , the fatigue limit of the material  $S_e = 0.5S_u$ , and  $S_u$  is the tensile strength of the base materials. The S–N relations for SPCC steel sheet, investigated in the present work, can be determined. When fatigue load is applied to the laser-welded lap joint, the resultant multi-axial stress distribution, including residual stress effects, can be determined via numerical simulation. To obtain the equivalent uniaxial stress corresponding to the multi-axial stress state, Sine’s method was used [11]. The equation for the equivalent uniaxial stress is as follows:

$$[(\sigma_1 - \sigma_2)^2 + (\sigma_2 - \sigma_3)^2 + (\sigma_3 - \sigma_1)^2]^{1/2} + m(\sigma_{m1} + \sigma_{m2} + \sigma_{m3}) = \sqrt{2} \frac{S_N}{K}$$

where  $\sigma_1, \sigma_2$ , and  $\sigma_3$  are the alternating components of stress and  $\sigma_{m1}, \sigma_{m2}$  and  $\sigma_{m3}$  are the mean components of stress.  $m$  is the coefficient of mean stress influence (0:25),  $K$  is the fatigue notch factor (1:4) and  $S_N$  is the uniaxial full reversed fatigue stress that is expected to give the same life as the multi-axial stress state for smooth specimens.

Substituting the values of alternating and mean stresses, which are obtained by finite element analysis, into Eq. (3), the uniaxial fatigue stress  $S_N$  can be obtained.

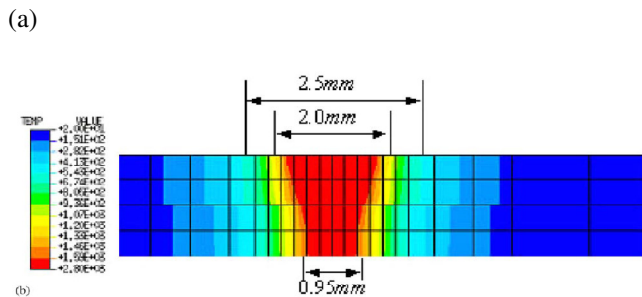
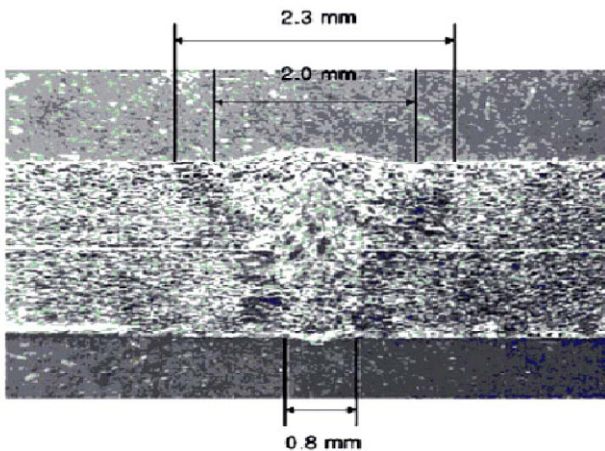


Fig. 4. Comparison of fusion zone (FZ) and heat affected zone (HAZ): (a) microstructure image, (b) FEM analysis.

**Fatigue test**

Two types of specimens were employed for the welding and the fatigue tests. The first is the transverse directional laser-welded specimen, which is perpendicular to fatigue load, using 1 mm thick SPCC sheets. The second is the longitudinal directional laser-welded specimen, which is parallel to fatigue load. For these two types of specimens, a tensile shear fatigue test was performed. Schematic diagrams of the tensile shear specimens are shown in Fig. 1. To remove notch effect of specimen generated from shearing, the milling process is done on the side of specimen. The fatigue test is run by axial load control at a stress ratio  $R = 0$  on an electro-hydraulic fatigue test machine of the INSTRON 2200 with a capacity of  $\pm 20$  kN. The basic load waveform is of sine wave type, and the repetition rate of the basic load waveform is 10 Hz. Fatigue life is defined as the cycle number during which a specimen becomes divided into two parts, and the fatigue limit is considered to be  $10^6$  cycles.

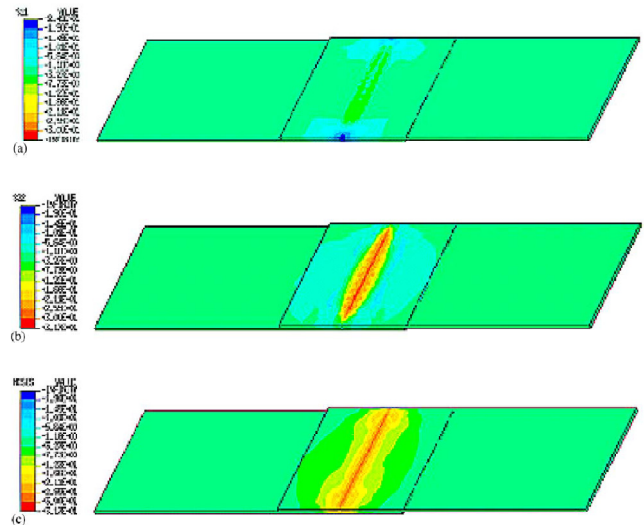


Fig.5. Stress distribution after laser welding of transverse direction: (a) x-direction residual stress ( $\sigma_x$ ;  $\text{kgf/mm}^2$ ), (b) y-direction residual stress ( $\sigma_y$ ;  $\text{kgf/mm}^2$ ), (c) von Mises stress ( $\text{kgf/mm}^2$ ).

**4. RESULTS AND DISCUSSION**

Heat flow analysis and stress analysis were performed for the welding direction using finite element analysis; longitudinal direction and transverse direction govern the same fatigue loading. Fig. 4(a) shows the microstructure image of the welded cross section. The result of heat flow analysis at 0:5 s in the welded cross section is shown in Fig. 4(b). Heat flow analysis in the fusion zone and heat affected zone agrees with experimental result as shown in Fig. 4. From the results of transient heat flow analysis, the residual stress distribution is evaluated. Figs. 5 and 6 show the residual stress distributions for welding direction in the lap joint with a 1 mm thick plate.



Direction (transverse direction welding—y-axis, longitudinal direction—x-axis shown in Fig. 2) parallel to welding bead shows tensile residual stress up to yield strength. Fig. 7 indicates von Mises stress distribution, while considering residual stress. When a fatigue load is applied to two types, the two cases show von

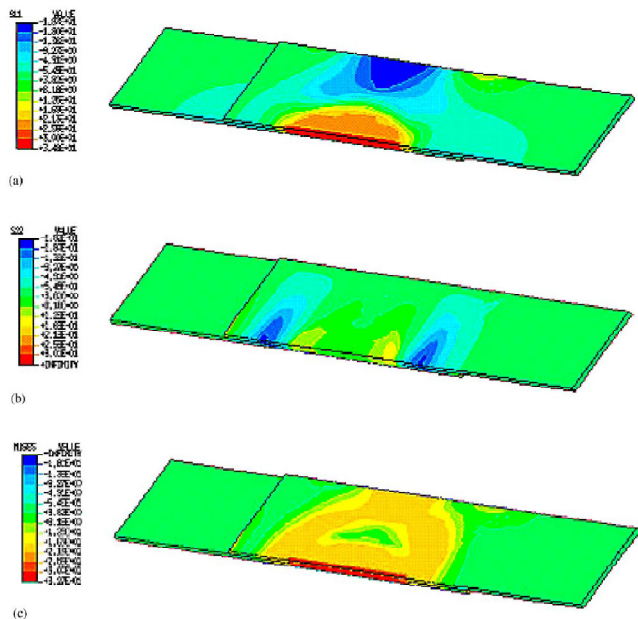


**Fig. 6. Stress distribution after laser welding of longitudinal direction: (a) x-direction residual stress ( $\sigma_x$ ;  $\text{kgf/mm}^2$ ), (b) y-direction residual stress ( $\sigma_y$ ;  $\text{kgf/mm}^2$ ), (c) von Mises stress ( $\text{kgf/mm}^2$ ).**

Mises stress distribution, with residual stress effect being higher than that neglecting the residual stress effect in Fig. 7. When a fatigue load is applied to the laser-welded lap joint, the resultant multi-axial stress distribution in lap joint, including residual stress effect, is determined via numerical simulation. The equivalent fatigue stress is calculated at the point initiating the fatigue failure in lap joint. The equivalent fatigue stress of laser-welded lap joint is calculated by substituting the resultant multi-axial stress by considering the residual stress effect into Eq. (2) via Sine's method. The fatigue life versus fatigue load curves, which include experimental data, are shown in Fig. 8. In Fig. 8, the calculated fatigue lives with the residual stress effect match the results of experiment. Comparison of the calculated fatigue life obtained, considering the residual stress effect with experimental data, shows the accuracy and validity of the calculations. It is evident that residual stress near the weld is a major factor affecting fatigue life. The welding length of transverse direction welding is 40 mm and that of longitudinal direction is 60 mm. Therefore, it is necessary to select a basis to compare the fatigue strength in regard to the welding direction.

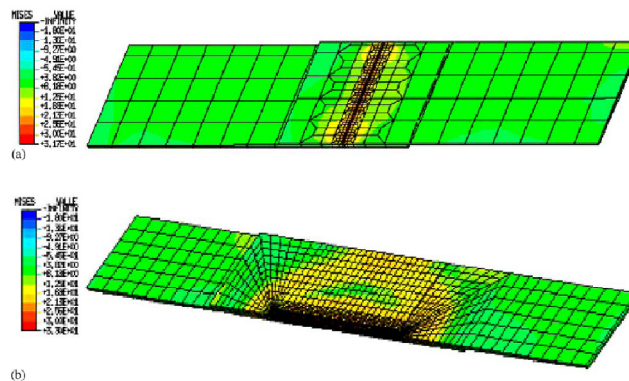


**Fig. 7. Stress distribution for tensile shear loading (200 kgf) with residual stress effect: (a) von Mises stress of transverse direction welding ( $\text{kgf/mm}^2$ ), (b) von Mises stress of longitudinal direction welding ( $\text{kgf/mm}^2$ ).**

The finite element mesh with the equal welding length is modeled and calculation of fatigue lives is carried out. In Fig. 9 the predicted fatigue life using the proposed method via Sine's method, is compared to the different welding directions under the same fatigue loading. In longitudinal welding direction, the calculated fatigue strength including the residual stress effect is lower than that of transverse direction because only the two tips of the longitudinal welding direction take up most of the load whereas the load is shared by the two sides of the transverse welding direction. The direction of tensile residual stress up to yield strength is similar to the weld line. Therefore, this implies that the fatigue load in the direction of the tensile residual stress decreases the fatigue strength of the weldment. It is also evident that welding direction is a major factor affecting fatigue life.

## 5. CONCLUSION

Heat flow analysis and stress analysis, for two types of laser-welded lap joints with different welding directions under the same fatigue loading direction, are performed using the finite element method. In addition, fatigue life including the residual stress effect is estimated from equivalent uniaxial fatigue stress, which is obtained using Sine's method. A comparison of the calculated fatigue strength with experimental data shows the validity and accuracy of the proposed method. Making use of the above result, the S-N curve of the laser-welded lap joint with different welding directions can be predicted. The summary of the conclusions is shown below.

Residual stress distributions for two types of laser-welded lap joints with different welding directions can be found using finite element method, indicating that the maximum tensile residual stress is identical to the order of yield strength. Fatigue life including the residual stress effect is estimated and this agrees with the experimental results of fatigue test.

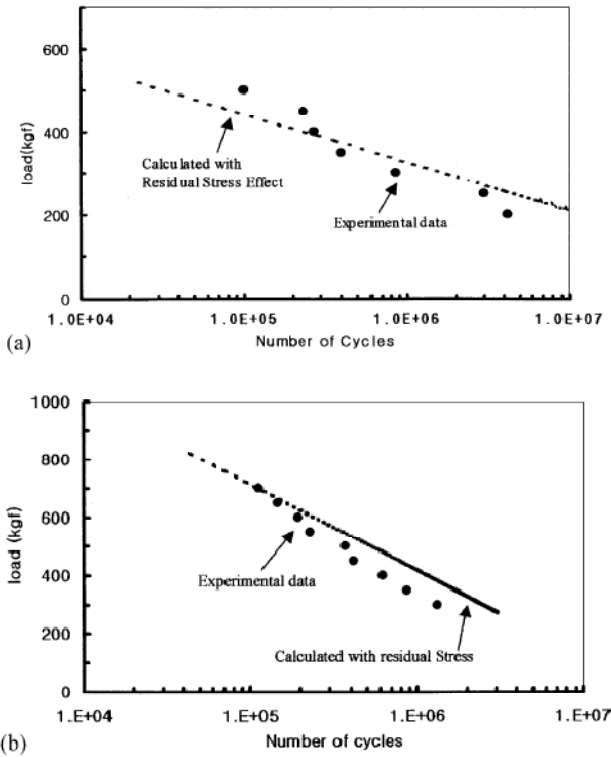


**Fig. 8. Experimental and calculated fatigue strength: (a) fatigue strength of transverse direction welding, (b) fatigue strength of longitudinal direction welding.**

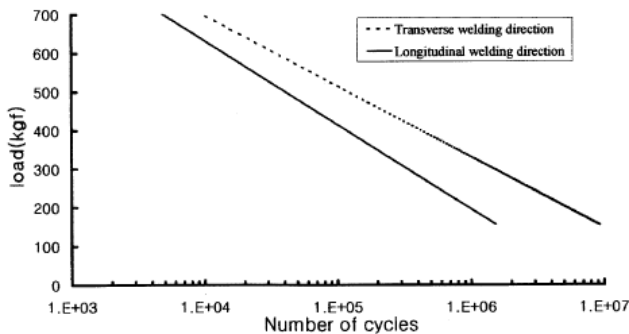


**Fig. 9. Comparison of calculated fatigue strength for longitudinal direction welding and transverse direction welding.**

Also Concentrating on the application of manufacturing technology, it is economically advantageous to use the proposed method to predict fatigue life, using finite element method in costs and time. The fatigue strength of the transverse lap laser-welded joint is higher than that of the longitudinal lap laser-welded joint.

**REFERENCES**

- [1] J.K. Baysore, M.S. Williamson, Y. Adonyi, J.L. Milian, Laser beam welding and formability of tailored blanks, *Weld. J.* 74 (1995) 345–352.
- [2] S.J. Maddox, *Fatigue Strength of Welded Structures*, The Welding Institute, 2nd Edition, Abington publishing, Cambridge, England, 1911.
- [3] E. Grotke, Indirect tests for weldability, in: R.D. Stout, W.D. Doty (Eds.), *Weldability of Steels*, Welding Research Council, New York, 1978.
- [4] J.W. Fisher, et al., Effect of weldments on the fatigue strength of steel beams, NCHRP Report 102, Transportation Research Board, Washington DC, 1970.
- [5] Y.S. Yang, K.-J. Son, S.-K. Cho, S.-G Hong, S.-K. Kim, K.-H. Mo, Effect of residual stress on fatigue strength of resistance spot weldment, *Sci. Technol. Weld. Joi.* 6 (2001) 397–401.
- [6] N.T. Ninh, M.A. Wahab, The effect of residual stresses and weld geometry on the improvement of fatigue life, *J. Mater. Process. Technol.* 48 (1995) 581–588.
- [7] K. Masubuchi, Models of stresses and deformations due to welding—A review, *J. Met.* 33 (1981) 19–23.
- [8] ABAQUS/Standard User’s Manual Version 6.1, Hibbit, Karlsson & Sorensen, Inc., RI, 2000.
- [9] J.R. Davis et al., *Metals Handbook*, Vol. 1, 10th Edition, American Society for Metals, Materials Park, 1990, pp. 195–199.
- [10] J.A. Bannantine, J.J. Comer, J.L. Handrock, *Fundamentals of Metal Fatigue Analysis*, Prentice-Hall, EnglewoodCliffs, NJ, 1990.
- [11] H.O. Funchs, R.I. Stephens, *Metal Fatigue in Engineering*, Wiley, New York, 1980.